SCIENTIFIC REPORTS

OPEN

SUBJECT AREAS:
MOLECULAR EVOLUTION
NUCLEIC ACIDS
TRANSCRIPTION

Received
24 September 2013

Accepted
26 November 2013

Published
11 December 2013

Correspondence and requests for materials should be addressed to K.W. (wakasugi@bio.c.u-tokyo.ac.jp)

Expression of the rodent-specific alternative splice variant of tryptophanyl-tRNA synthetase in murine tissues and cells

Miki Miyanokoshi[1], Tomoaki Tanaka[1], Miho Tamai[2], Yoh-ichi Tagawa[2] & Keisuke Wakasugi[1]

[1]Department of Life Sciences, Graduate School of Arts and Sciences, The University of Tokyo, 3-8-1 Komaba, Meguro-ku, Tokyo 153-8902, Japan, [2]Department of Biomolecular Engineering, Graduate School of Bioscience and Biotechnology, Tokyo Institute of Technology, 4259 B51 Nagatsuta-cho, Midori-ku, Yokohama, Kanagawa 226-8501, Japan.

Tryptophanyl-tRNA synthetase (TrpRS) catalyzes the aminoacylation of $tRNA^{Trp}$. mRNA of a rodent-specific alternative splice variant of TrpRS (SV-TrpRS), which results in the inclusion of an additional hexapeptide at the C-terminus of full-length TrpRS (FL-TrpRS), has been identified in murine embryonic stem (ES) cells. In the present study, we evaluated the expression of mouse TrpRS mRNA by real-time reverse transcription PCR. We show that SV-TrpRS and FL-TrpRS mRNAs are highly expressed in murine ES cells, embryo, spleen, lung, liver and uterus, and that the relative expression of SV-TrpRS compared to FL-TrpRS is significantly less in the brain. Moreover, we found that interferon-γ increases the expression of TrpRS in a mouse cell line. These results provide the first evidence for tissue-specific expression and alternative splicing of mouse TrpRS.

Aminoacyl-tRNA synthetases are key enzymes in the process of protein biosynthesis and catalyze the aminoacylation of their cognate tRNAs[1]. Tryptophanyl-tRNA synthetase (TrpRS) catalyzes activation of tryptophan (Trp) by ATP and transfer to $tRNA^{Trp}$. Mammalian TrpRSs contain an additional domain at the N-terminus that is absent from lower eukaryotic and prokaryotic TrpRSs[2]. In human cells, TrpRS exists in two forms: a major form representing the full-length protein (a.a. 1–471), and a truncated form (mini TrpRS) (a.a. 48–471) in which most of the N-terminal extension (a.a. 1–47) is deleted because of alternative splicing of the pre-mRNA[2–5]. Human full-length and mini TrpRSs can catalyze the aminoacylation of $tRNA^{Trp}$[6,7]. Moreover, human mini TrpRS exhibits angiostatic activity, whereas the full-length enzyme does not[6,8,9].

In murine embryonic stem (ES) cells, rodent-specific alternative splicing of TrpRS has been reported[10]. Mouse full-length TrpRS (FL-TrpRS: a.a. 1–475) is produced by normal splicing and is similar in molecular weight to the full-length TrpRSs from other mammals. Alternative splicing of mouse TrpRS mRNA generates an alternative splice variant (SV-TrpRS: a.a. 1–481), that contains an additional hexapeptide, Cys-Phe-Cys-Phe-Asp-Thr, at the C-terminus of mouse FL-TrpRS[10].

In the present study, we first designed primers to discriminate between mRNAs corresponding to murine FL-TrpRS and SV-TrpRS. We used these primers to perform real-time reverse transcription PCR (RT-PCR) to evaluate the relative expression of the FL-TrpRS and SV-TrpRS mRNA in murine ES cells, tissues, and cell lines. We show that SV-TrpRS and FL-TrpRS are highly expressed in most of the samples we analyzed. Moreover, because the expression of human TrpRS has been reported to be strongly increased in response to interferon (IFN)-γ[5,11–14], we also analyzed the effects of IFN-γ on the expression of mouse TrpRS. We found that TrpRS mRNA and protein are increased in a murine cell line following exposure to IFN-γ.

Results

Detection of mouse FL-TrpRS and SV-TrpRS by real-time RT-PCR. In the present study, to investigate the expression of mouse FL-TrpRS and SV-TrpRS by real-time RT-PCR, we first designed primers specific to FL-TrpRS and SV-TrpRS mRNAs. As shown in Fig. 1A and Table I, to detect the total amount of mouse FL-TrpRS and SV-TrpRS mRNAs, we designed total TrpRS forward (Fw) and reverse (Rv) primers, which can amplify the common coding region of mouse TrpRSs mRNAs. Moreover, to analyze only the expression of SV-TrpRS mRNA,

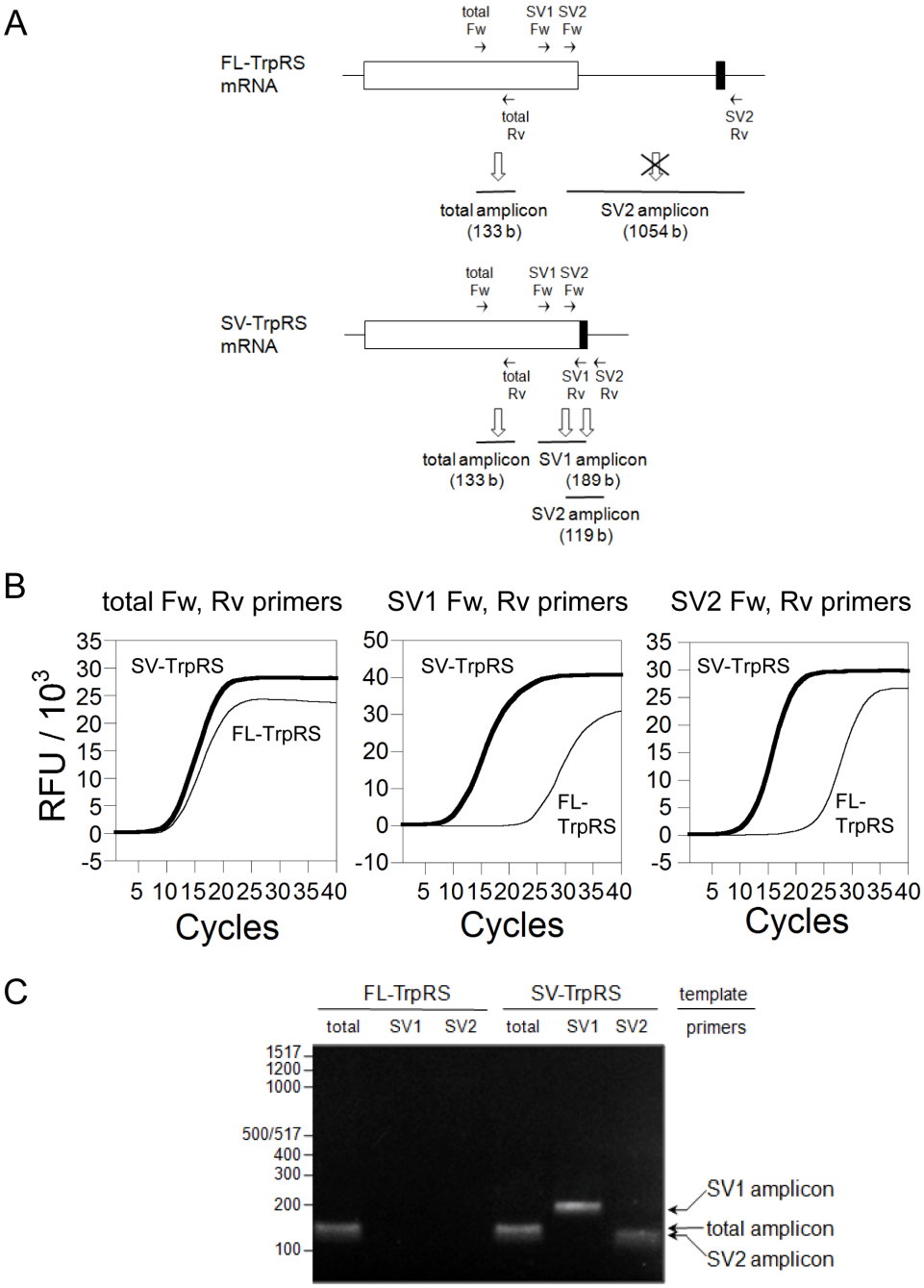

Figure 1 | Detection of mouse FL-TrpRS and SV-TrpRS mRNA by real-time RT-PCR. (A) Schematic illustration of mouse TrpRS mRNAs. The open box indicates the location of the common open reading frame encoding mouse FL-TrpRS. The closed box indicates the alternatively translated sequence. The total TrpRS Fw and Rv primers, SV1 TrpRS Fw and Rv primers, and SV2 TrpRS Fw and Rv primers are indicated at their proper positions. Total TrpRS Fw and Rv primers are used to amplify both mouse FL-TrpRS and SV-TrpRS mRNAs. SV1 or SV2 Fw and Rv primers can amplify mouse SV-TrpRS mRNA preferentially. (B) Real-time PCR amplification plots of mouse FL-TrpRS and SV-TrpRS. Plasmid vectors containing the mouse FL-TrpRS (fine line) or SV-TrpRS (bold line) cDNA were used as templates. Total TrpRS Fw and Rv primers, SV1 TrpRS Fw and Rv primers, or SV2 TrpRS Fw and Rv primers were used for each experiment. Data represents a typical real-time PCR output. RFU, relative fluorescence units. (C) The RT-PCR products after 14 cycles of amplification were analyzed by 2% agarose gel electrophoresis and staining with ethidium bromide. DNA molecular size markers (100–1517 bp) are shown on the left. Arrows indicate the positions of the PCR products. Plasmid vectors containing the mouse FL-TrpRS or SV-TrpRS cDNA were used as templates. PCR was performed using total TrpRS Fw and Rv primer set, SV1 TrpRS Fw and Rv primer set, or SV2 TrpRS Fw and Rv primer set.

two strategies using different primer sets were performed. (i) As shown in Table I and Fig. 1A, the SV1 TrpRS Rv primer is a 21-mer oligonucleotide, which contains 7 nucleotides complementary to the common C-terminal sequence of mouse TrpRSs and 14 nucleotides complementary to the alternatively spliced coding sequence specific to mouse SV-TrpRS mRNA. SV-TrpRS mRNA is amplified preferentially by using the SV1 TrpRS Fw and Rv primer set. (ii) the SV2 TrpRS Rv primer is located in the 3′ untranslated sequence (Table I and Fig. 1A). Under the RT-PCR experimental conditions used, the SV2 TrpRS Fw and Rv primer set can amplify the SV-TrpRS mRNA but not the FL-TrpRS mRNA because the PCR product generated from the FL-TrpRS mRNA using the SV2

Table I | Primers used for RT-PCR

Primer name	Sequence
Total TrpRS Fw primer	5′-GAAAGGCATTTTCGGCTTTACG-3′
Total TrpRS Rv primer	5′-GATGAGGCACTGGATATCTG-3′
SV1 TrpRS Fw primer	5′-GGAGCAGATCAGAAAGGATTAC-3′
SV1 TrpRS Rv primer	5′-TCAAAGCAGAAGCACTGGAAG-3′
SV2 TrpRS Fw primer	5′-CTGTCCTTCCACTTCCAG-3′
SV2 TrpRS Rv primer	5′-CTGCTGTTCTTTTCTGTCTAG-3′
HPRT Fw primer	5′-ATACAGGCCAGACTTTGTTGG-3′
HPRT Rv primer	5′-CAACTTGCGCTCATCTTAGG-3′

TrpRS Fw and Rv primer set is too long (1054 b) for successful amplification.

First, to check the specificity of the primers for real-time RT-PCR, two plasmid vectors carrying the mouse FL-TrpRS (Clone ID 6813406; Genbank Accession number BC046232) or SV-TrpRS (Clone ID 2654231; Genbank Accession number BC003450) cDNA were used as templates (Fig. 1A). When the total TrpRS Fw and Rv primer set was used, both vectors were amplified with the same threshold cycle (Ct) values (Fig. 1B). In contrast, when the SV1 or SV2 TrpRS Fw and Rv primer set was used, the vector containing the mouse SV-TrpRS was amplified preferentially (Fig. 1B). Moreover, Fig. 1B shows that the Ct values obtained when using the SV1 or SV2 TrpRS primer set was similar to that obtained when using the total TrpRS primer set.

The amplified products were electrophoresed through a 2% agarose gel stained with ethidium bromide. Amplification of the FL-TrpRS and SV-TrpRS templates with the total TrpRS Fw and Rv primer set generated the predicted products of approximately 133 b (Fig. 1C). As shown in Fig. 1C, the specific amplification of SV-TrpRS using the SV1 TrpRS primer set and SV2 TrpRS primer set generated the predicted unique amplification products of 189 b and 119 b, respectively.

Expression of FL-TrpRS and SV-TrpRS mRNAs in murine ES cells and tissues. We compared the expression of FL-TrpRS and SV-TrpRS mRNAs in murine ES cells and brain by real-time RT-PCR. A PCR primer set for the housekeeping gene hypoxanthine-guanine phosphoribosyltransferase (HPRT) (HPRT Fw and Rv) was used for normalization. The relative expression of TrpRS mRNAs compared to the HPRT mRNA in ES cells are expressed as a ratio of the corresponding values in the brain (Figs. 2A–2C). The expression of total TrpRS (FL-TrpRS + SV-TrpRS) mRNAs in murine ES cells is twice that observed in the brain (Fig. 2A). Figs. 2B and 2C show that SV-TrpRS mRNA is highly expressed in murine ES cells and that its expression is significantly reduced in mouse brain.

The *in vitro* hepatic organogenesis model derived from murine ES cells exhibited high levels of multiple hepatic functions[15,16]. We therefore next differentiated the murine ES cells, ST1 and E14.1 cells, into liver-like tissues and analyzed the expression of mouse TrpRS mRNA 18 days after plating (A18). As shown in Fig. 2, the expression of SV-TrpRS and FL-TrpRS mRNAs in the *in vitro* organogenesis model was similar to that observed in murine ES cells, suggesting that the expression of FL-TrpRS and SV-TrpRS mRNAs does not vary with the stage of differentiation of mouse ES cells.

We next analyzed the expression of FL-TrpRS and SV-TrpRS mRNAs in the murine embryo and other tissues by real-time RT-PCR. FL-TrpRS mRNA was ubiquitously expressed with a relatively high abundance in murine embryo, spleen, lung, liver, and uterus (Fig. 3A). As shown in Figs. 3B and 3C, we observed that SV-TrpRS mRNA was highly expressed in murine embryo, spleen, lung, liver, and uterus, but observed weak expression in the brain.

Effects of IFN-γ on the expression of mouse TrpRS. Because TrpRS mRNA has been reported to increase approximately 40–60 fold in human cells exposed to IFN-γ[12], we next compared the level of mouse FL-TrpRS and SV-TrpRS mRNAs in the mouse cell lines, Hepa 1–6 and RAW 264 in the absence or presence of IFN-γ. Expression of both SV-TrpRS and FL-TrpRS mRNA was increased in Hepa 1–6 cells following exposure to IFN-γ (Fig. 4). In contrast, the expression of mouse FL-TrpRS and SV-TrpRS mRNAs remained unchanged in RAW 264 cells following exposure to IFN-γ (Fig. 4).

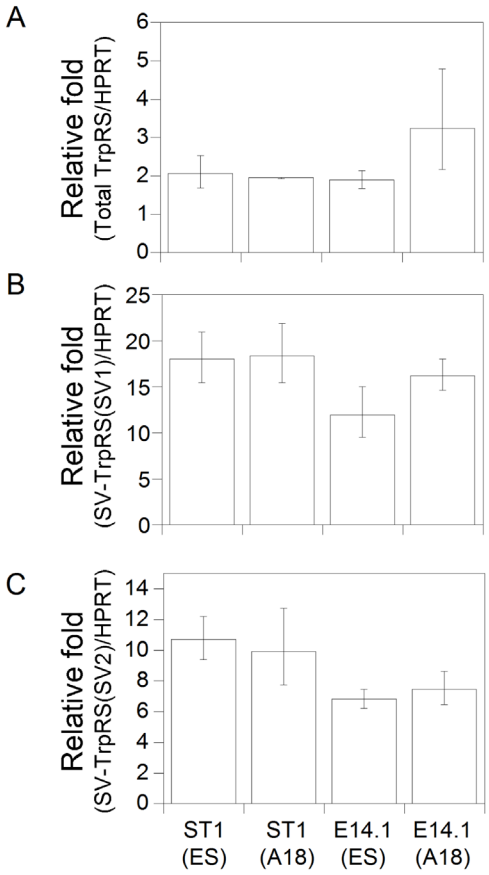

Figure 2 | Comparison of the expression of FL-TrpRS and SV-TrpRS mRNAs in murine ST1 and E14.1 ES cell lines and their differentiated progeny. Expression of TrpRS mRNA was determined relative to HPRT by real-time RT-PCR and normalized to the brain sample using the $2^{-\Delta\Delta Ct}$ method. Data represent the means from at least three or more independent experiments, each carried out in duplicate, error bar = standard deviation (SD). (A) Relative expression of the total TrpRS (FL-TrpRS and SV-TrpRS)/HPRT. (B) Relative expression of SV-TrpRS (monitored by SV1 primers)/HPRT. (C) Relative expression of SV-TrpRS (monitored by SV2 primers)/HPRT.

We next evaluated the specificity of an antibody to detect expression of mouse TrpRS proteins. Vectors encoding either mouse FL-TrpRS or SV-TrpRS protein fused to an N-terminal 6xHis-tag (pcDNA4/HisMax©-TOPO®-mouse FL-TrpRS expression vector and pcDNA4/HisMax©-TOPO®-mouse SV-TrpRS expression vector, respectively) were transfected into murine Hepa 1–6 cells and Western blot analyses of the transfected cell extracts were performed using anti-TrpRS, anti-6xHis-tag, and anti-β-actin antibodies. β-actin was used as a loading control. As shown in Fig. 5A, molecular weights of the polypeptides detected by anti-TrpRS antibodies were indistinguishable from those detected by the anti-6xHis-tag antibody, indicating that the anti-TrpRS antibody recognizes mouse TrpRS specifically. Fig. 5A also shows that the band of 6xHis-tagged mouse SV-TrpRS was detected at the same molecular weight as that of 6xHis-tagged mouse FL-TrpRS. We then analyzed the effects of IFN-γ on the level of mouse TrpRS protein in mouse Hepa 1–6 cells

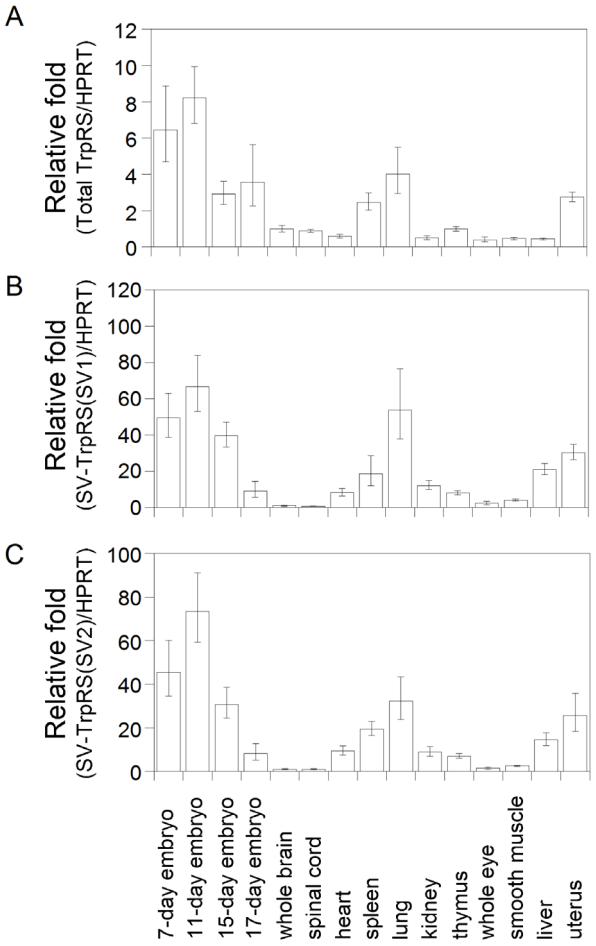

Figure 3 | Comparion of the expression of FL-TrpRS and SV-TrpRS mRNAs in murine embryo and several tissues. Expression of TrpRS mRNA was determined relative to HPRT by real-time RT-PCR and normalized to that in the brain sample using the $2^{-\Delta\Delta Ct}$ method. Experiments were performed in triplicate; error bar = SD. (A) Relative expression of the total TrpRS/HPRT. (B) Relative expression of SV-TrpRS (monitored by SV1 primers)/HPRT. (C) Relative expression of SV-TrpRS (monitored by SV2 primers)/HPRT.

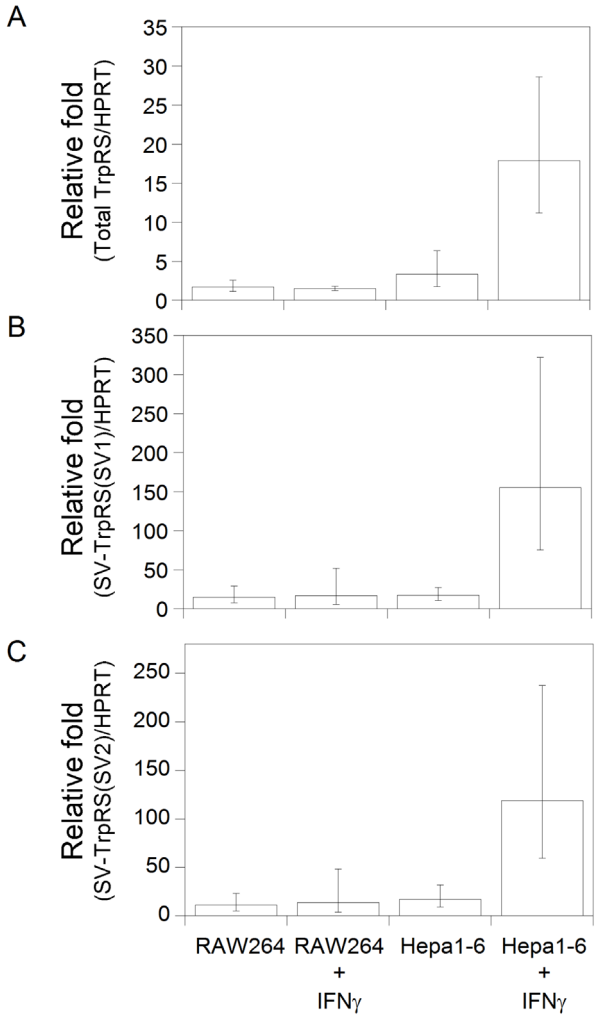

Figure 4 | Comparison of the expression of FL-TrpRS and SV-TrpRS mRNAs in murine cell lines Hepa1–6 and RAW264 in the absence or presence of IFN-γ. Expression of TrpRS mRNA was determined relative to HPRT by real-time RT-PCR and normalized to that observed in the brain sample using the $2^{-\Delta\Delta Ct}$ method. All data are derived from at least three or more independent experiments, each carried out in duplicate; error bar = SD. (A) Relative expression of the total TrpRS/HPRT. (B) Relative expression of SV-TrpRS (monitored by SV1 primers)/HPRT. (C) Relative expression of SV-TrpRS (monitored by SV2 primers)/HPRT.

using the anti-TrpRS antibody and observed that expression of mouse TrpRS protein is increased significantly in response to IFN-γ (Fig. 5B). Taken together, we conclude that IFN-γ increases mRNA expression and protein production of TrpRS in mouse Hepa 1–6 cells. On the other hand, the expression of mouse TrpRS protein did not change in RAW 264 cells following exposure to IFN-γ (Fig. 5C). This result is consistent with that of TrpRS mRNA in RAW 264 cells by RT-PCR.

Discussion

In the present study, we show that FL-TrpRS and SV-TrpRS mRNAs are highly expressed in murine ES cells and several tissues such as spleen, lung, liver, and uterus and that the relative expression of SV-TrpRS compared to FL-TrpRS is significantly less in the brain. Because the amplification efficiencies of the SV1 TrpRS and SV2 TrpRS primer sets were similar to that of the total TrpRS primer set, we estimated the ratio of SV-TrpRS to total TrpRS (FL-TrpRS + SV-TrpRS) based on the C_t values of SV-TrpRS and total TrpRS. According to this analysis, the percentage of SV-TrpRS in the total TrpRS is less than 0.7% in mouse brain and is approximately 6% in mouse ES cells. This result is consistent with the previous data of Northern blot analyses of mouse FL-TrpRS and SV-TrpRS expression[10].

Previously, the gene expression profile of human TrpRS present in a human transcriptome database revealed a striking overexpression in placenta, lung, and spleen[17]. The expression patterns of mouse FL-TrpRS and SV-TrpRS are similar to that of human full-length TrpRS, although the differences among the expression levels of TrpRS in mouse tissues are smaller than those among human tissues[17]. Moreover, we found that the expression of mouse TrpRS is increased in a cell line following exposure to IFN-γ. Previous analysis of human TrpRS expression in response to IFN-γ showed that human TrpRS mRNA is increased approximately 50-fold in response to IFN-γ[12], suggesting that the induction of murine TrpRS is less than occurs in human cells. Because the expression of both mouse and human TrpRSs is increased by IFN-γ, the similar tissue-specific expression patterns of mouse and human TrpRSs is not surprising. Another representative IFN-γ-inducible enzyme is indoleamine 2,3-dioxygenase (IDO)[18,19]. IDO is responsible for Trp degradation, and it catalyzes the first as well as the rate-limiting step in the major pathway of Trp metabolism, the kynurenine pathway[20]. High levels of IDO expression have been detected in several murine tissues such as

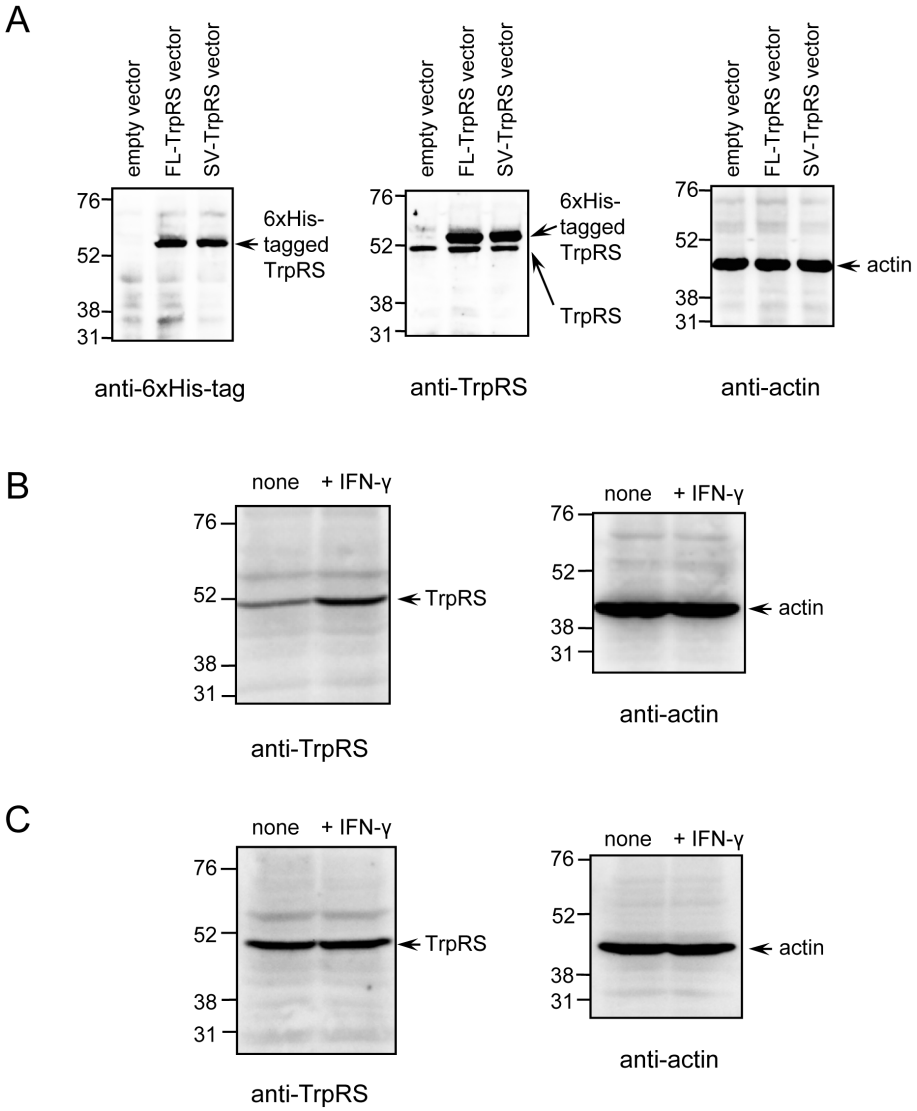

Figure 5 | Western blot analyses of TrpRS in murine cell extracts. Samples were analyzed on 12.0% SDS-polyacrylamide gels and by Western blot analyses using anti-6xHis-tag, anti-TrpRS, or anti-β-actin antibodies. Molecular size markers (in kilodaltons) are shown on the left. (A) Western blot analysis of mouse TrpRS with 6xHis-tag. pcDNA4/HisMax©-TOPO®-mouse TrpRS expression vector or empty vector was transfected into Hepa 1–6 cell lines. (B) Western blot analysis of mouse TrpRS in cell extracts from Hepa 1–6 in the absence or presence of IFN-γ. (C) Western blot analysis of mouse TrpRS in cell extracts from RAW 264 in the absence or presence of IFN-γ.

spleen and lung[21]. It has been suggested that IDO-expressing cells avoid self-destruction resulting from Trp depletion by a concomitant increase in the expression of TrpRS[22]. Overexpression of TrpRS in the cell could facilitate production of a pool of Trp-tRNA, thus providing a reservoir for Trp that would be protected from degradation by IDO and therefore available for protein synthesis.

IFN-γ is a central regulator of the immune response and signals[23,24]. Gamma Activation Sequences (GAS) and interferon-stimulated response elements (ISRE) are important during IFNγ-mediated gene expression[23,24]. Genomic DNA organization and alternative splicing of the mouse TrpRS are summarized in Fig. 6A. Two transcription start sites (P1 and P2) are presumed on the basis of the data of the NCBI and Ensembl databases (Fig. 6A). Processing of the primary transcript initiated from the P1 start site generates the mRNA isoform where exon Ia joins to exon II. The other two isoforms are produced by alternative splicing of the primary transcript produced from the P2 start site. As listed in Fig. 6B, we identified GAS and ISRE candidate sequences between the P1 and P2 start sites. The consensus sequences of GAS and ISRE are defined as TTC/ANNNG/TAA and NGAAANNGAAAG/CN, where N represents any nucleotide, respectively[23,24]. Further studies to investigate IFNγ-mediated regulation of mouse TrpRS and brain-specific suppression of the alternative splicing of mouse TrpRS are underway.

In the present study, we found that SV-TrpRS mRNA is expressed in murine embryo and many tissues as well as ES cells. Moreover, we showed that IFN-γ enhances expression of TrpRS in mouse Hepa 1–6 cells. To our knowledge, no such alternative splicing as mouse TrpRS mRNA has yet been described in lower and higher vertebrates. The tissue-specific distribution pattern and IFN-γ-mediated upregulation of mouse SV-TrpRS imply the functional importance of SV-TrpRS.

We previously revealed species-specific differences in the regulation of the aminoacylation activity of mammalian TrpRSs[25,26]. We found that human TrpRS binds Zn^{2+} or an iron protoporphyrin IX complex (heme), which enhances its aminoacylation activity and showed that Zn^{2+}-depleted human TrpRS is enzymatically inactive and that binding of Zn^{2+} or heme to human TrpRS stimulates its aminoacylation activity[25]. Moreover, we demonstrated that when expression of human TrpRS is increased in response to IFN-γ, some of the newly produced TrpRS protein is in the Zn^{2+}-free form, such

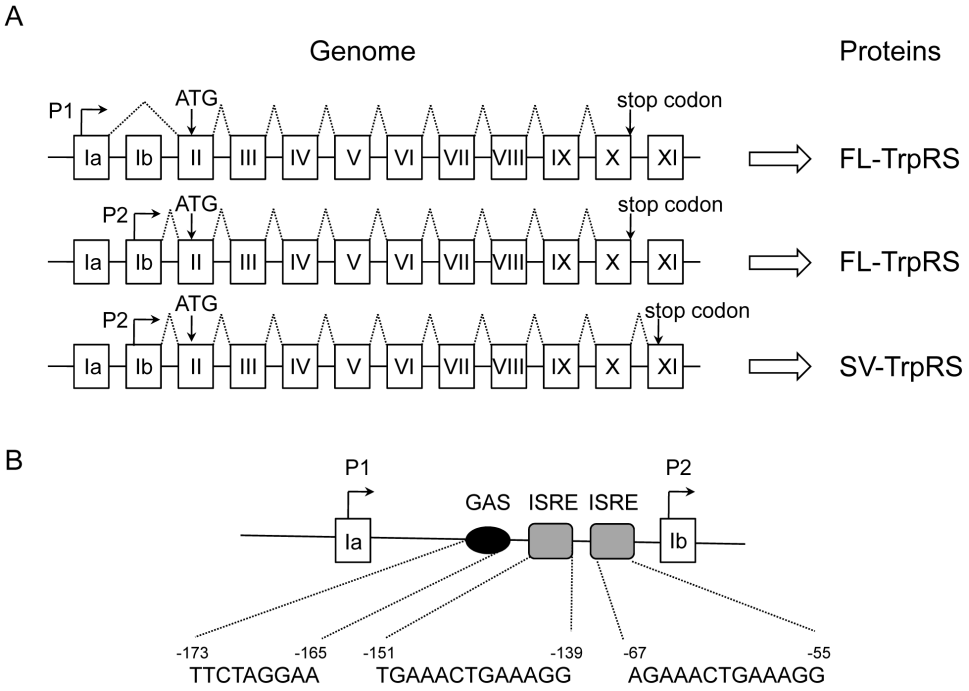

Figure 6 | Schematic representation of the mouse TrpRS gene. (A) Genomic DNA organization and alternative splicing of the mouse TrpRS gene, which are based on the data of the NCBI and Ensembl databases. Open boxes and lines represent exons and introns, respectively. Discontinuous lines indicate spliced forms of TrpRS mRNA. The positions of the ATG start codon and stop codon are indicated by arrows. The presumed two transcription start sites are shown as P1 and P2. (B) Schematic representation of the 5′ regulatory region of mouse TrpRS. The presumed transcription start site within exon Ib is referred to as +1. The putative IFN-γ regulatory elements and their nucleotide sequences and positions are indicated. The presumed two transcription start sites are indicated as P1 and P2. GAS, Gamma Activation Sequence; ISRE, Interferon-stimulated Response Element.

that the aminoacylation activity of this new protein is therefore sensitive to the level of heme or Zn^{2+} [25]. In contrast, we found that mouse FL-TrpRS and bovine TrpRS are constitutively active regardless of the presence of Zn^{2+} or heme[26]. Because the two Cys and Asp residues in the C-terminal sequence specific for mouse SV-TrpRS, CFCFDT, might form a metal-binding site, further studies are in progress to investigate whether the enzymatic activity of mouse SV-TrpRS is regulated by metal ions such as Zn^{2+} and/or heme as is the case for human TrpRS, the expression of which is up-regulated by IFN-γ. Moreover, because the CFCFDT sequence of mouse SV-TrpRS is similar to the C-terminal sequence found in Ras proteins and γ-subunits of heterotrimeric G proteins[10], it might represent a site of membrane attachment via posttranslational modification such as isoprenylation, as is the case for Ras and the γ-subunits of G proteins. Further studies are necessary to investigate the physiological function of the rodent-specific SV-TrpRS.

Methods

Chemicals. A Mouse Total RNA Master Panel prepared from BALB/c mice (7-day embryo, 11-day embryo, whole brain, whole eye, heart, kidney, liver, lung, smooth muscle, spinal cord, spleen, thymus, and uterus) and Webster mice (15-day embryo and 17-day embryo) was purchased from CLONTECH Laboratories, Inc. (Palo Alto, CA). Plasmid vectors carrying a murine FL-TrpRS cDNA (Clone ID 6813406; Genbank Accession number BC046232) and an SV-TrpRS cDNA (Clone ID 2654231; Genbank Accession number BC003450) were purchased from Invitrogen (Carlsbad, CA). Recombinant rat IFN-γ was purchased from eBioscience (San Diego, CA).

Cell culture and reagents. The mouse ES cell line ST1 was originally established from the blastocyst of a BALB/c mouse, and it was transmitted through the germline in chimeric mice. ST1 and E14.1 mouse ES cells derived from 129/Ola mice were grown on a mitomycin C-treated feeder layer of primary cultures of mouse embryonic fibroblasts so as to maintain their undifferentiated state in Dulbecco's modified Eagle's medium (DMEM) (Invitrogen) containing 20% fetal bovine serum (FBS) (Nichirei Biosciences, Tokyo, Japan), 1 mM sodium pyruvate (Invitrogen), 0.1 mM nonessential amino acid (Invitrogen), 100 μM 2-mercaptoethanol (Sigma-Aldrich, St. Louis, MO), and 10^3 U/mL leukemia inhibitory factor (Chemicon, Temecula, CA).

A mouse hepatoma cell line, Hepa 1–6 (RCB1638), and a mouse macrophage cell line, RAW 264 (RCB0535), were obtained from the RIKEN Cell Bank (Tsukuba, Japan). These cells were cultured in DMEM containing 4.5 g/L of glucose, 10% (v/v) FBS, 100 U/ml of penicillin, 100 μg/ml of streptomycin, and 2 mM glutamine (all from Invitrogen) in a humidified atmosphere containing 5% CO_2 at 37°C. The medium was changed twice weekly, and the cultures were split 1 : 8 once every week.

Hepa 1–6 or RAW 264 cells were seeded at 4.0×10^5 cells/mL on CellBIND® Surface 35-mm cell culture dishes (Corning, Corning, NY) the day before experiments. The cells were treated with 100 Units/mL of IFN-γ (eBioscience) for 24 h at 37°C.

Differentiation of murine embryonic stem cells. The murine ES cell-derived hepatic tissue system was derived as described previously[15,16]. In brief, ST1 or E14.1 ES cells were dissociated with 0.25% trypsin solution and resuspended in Iscove's modified Dulbecco's medium (Invitrogen) containing 20% FBS, 1 mM sodium pyruvate, 100 μM nonessential amino acids, and 100 μM 2-mercaptoethanol and lacking leukemia inhibitory factor. The cells were cultured in a hanging drop (1000 cells per 50-μl drop) in an atmosphere of 5% CO2 at 37°C for 5 days. Under these conditions, cells formed embryoid bodies derived from ES cells. Fifty embryoid bodies were plated in a well of a gelatin-coated 6-well plate; the day of plating was denoted as day 0 (A0). In this study, murine ES cell-derived in vitro liver tissue model was used at A18. Cell differentiation was confirmed by monitoring downregulation of *oct3/4*, upregulation of hepatocyte-specific gene expression, and albumin protein production[15,16].

RNA isolation and cDNA synthesis. Total RNA from ST1 or E14.1 ES cells was isolated by the acid guanidinium isothiocyanate-phenol-chloroform-isoamyl alcohol method and genomic DNA was removed by treatment with DNase I (Promega, Madison, WI). Total RNA from Hepa 1–6 or RAW 264 cells was isolated by using an Aurum™ total RNA mini kit (BIO-RAD, Hercules, CA).

First-strand cDNA was synthesized from total RNA with Superscript II reverse transcriptase (Invitrogen) and an oligo$(dT)_{12-18}$ primer (Invitrogen) according to the manufacturer's protocols. The synthesized single-stranded cDNA was then treated with RNase H to remove RNA.

Primer design. The NCBI (National Center for Biotechnology Information [http://www.ncbi.nlm.nih.gov]) and Ensembl (Ensembl Genome Browser [http://www.ensembl.org/index.html]) databases were used to search for available mouse gene sequences to design primers using Primer3Plus [http://www.bioinformatics.nl/cgi-bin/primer3plus/primer3plus.cgi], taking into account possible secondary structures using Mfold [http://mfold.rna.albany.edu/?q=mfold]) and the specificity of the

primers using BLAST [http://blast.ncbi.nlm.nih.gov/]). Primer sequences prepared for RT-PCR are summarized in Table I.

Quantitative real-time PCR. Real-time PCR was performed in a Thermal Cycler CFX96™ real-time PCR detection system (BIO-RAD, Hercules, CA), using SsoFast™ EvaGreen® Supermix (BIO-RAD). Hypoxanthine-guanine phosphoribosyltransferase (HPRT) was used as an internal housekeeping reference. The PCR reactions using the HPRT Fw and Rv primer set or total TrpRS Fw and Rv primer set, which is listed in Table I, were initiated with a 30 sec incubation at 95.0°C, followed by 40 cycles of 95.0°C for 5 sec and 55.0°C for 20 sec. PCR reactions using the alternatively spliced SV1 or SV2 TrpRS Fw and Rv primer set, which is listed in Table I, were initiated with a 30 sec incubation at 95.0°C, followed by 40 cycles at 95.0°C for 5 sec and 55.7°C for 20 sec.

Data were analysed using the ΔC_t method. Briefly, target gene expression was normalized to the HPRT endogenous reference gene for each sample. The difference between mean threshold PCR cycle values for the target and HPRT genes generated the ΔC_t value. This was then calibrated to the control sample (brain) in each experiment to generate the $\Delta\Delta C_t$ value, where the brain control was assigned a $\Delta\Delta C_t$ value of 0. The fold target gene expression, compared to the calibrator value, is calculated using the formula $2^{-\Delta\Delta Ct}$. Error bars represent the standard deviation (SD) of each target gene value, after evaluating the expression $2^{-\Delta\Delta Ct+SD}$ and $2^{-\Delta\Delta Ct-SD}$, where SD is the standard deviation of the $\Delta\Delta C_t$ value.

A melting curve was performed at the end of the PCR run over the range of 65–95°C, increasing the temperature stepwise by 0.5°C every 5 sec. Gene-specific amplification was confirmed by a single peak in the melting-curve analysis and a single band on a 2% agarose gel stained with ethidium bromide.

Overexpression of mouse FL-TrpRS or SV-TrpRS by transfection of its expression vector. The nucleotide sequence of the cDNA coding for mouse FL-TrpRS or SV-TrpRS was cloned into the eukaryotic pcDNA4/HisMax©-TOPO® expression vector, which gives a gene product with a N-terminal tag of six histidine residues (6xHis-tag), by using the pcDNA4/HisMax©-TOPO® TA expression kit (Invitrogen) as directed by the manufacturer. The construct was confirmed by DNA sequencing (FASMAC Co., Ltd., DNA sequencing services, Atsugi, Japan). Hepa 1–6 cells were grown on a 25 cm^2 flask (Corning) until 70–80% confluence and were seeded at a density of 4.0×10^5 cells/mL in CellBIND® Surface 35-mm cell culture dishes (Corning) for 24 h. The pcDNA4/HisMax©-TOPO®-mouse TrpRS expression vector or control vector (empty vector) was transfected using Lipofectamine™ 2000 (Invitrogen) according to the manufacturer's instructions. After 24 h of transfection, the cells were collected.

Western blot analyses. Extracts of soluble proteins were resolved by electrophoresis through 12.0% polyacrylamide/sodium dodecyl sulfate (SDS) gels. For Western blot analyses, proteins were transferred onto Hybond-P PVDF membranes (GE Healthcare Biosciences, Piscataway, NJ), which were then blocked with 5% skim milk (Wako Pure Chemical Industries, Osaka, Japan). The membranes were incubated for 1 h with one of the following primary antibodies in phosphate-buffered saline (PBS): anti-TrpRS rabbit MaxPab® polyclonal antibodies (Abnova Co., Taipei, Taiwan) or anti-β-actin mouse monoclonal antibody (Sigma-Aldrich) or anti-penta-His mouse monoclonal antibody (Qiagen, Hilden, Germany). After being washed three times with PBS containing 0.1% Tween20, the membranes were incubated with an HRP-linked $F(ab')_2$ fragment of donkey anti-rabbit IgG or an HRP-linked sheep anti-mouse IgG (GE Healthcare Biosciences) for 1 h. The membrane was again washed three times with the buffer, and the proteins were visualized using ECL™ Western blotting detection reagents (GE Healthcare Biosciences). Chemiluminescent signals were detected using a LAS-4000 mini luminescent image analyzer (GE Healthcare Biosciences).

1. Schimmel, P. Aminoacyl-tRNA synthetases: General scheme of structure-functional relationships in the polypeptides and recognition of transfer RNAs. *Annu Rev Biochem.* **56**, 125–158 (1987).
2. Frolova, L. Y., Grigorieva, A. Y., Sudomoina, M. A. & Kisselev, L. L. The human gene encoding tryptophanyl-tRNA synthetase: interferon-response elements and exon-intron organization. *Gene.* **128**, 237–245 (1993).
3. Tolstrup, A. B., Bejder, A., Fleckner, J. & Justesen, J. Transcriptional regulation of the interferon-γ-inducible tryptophanyl-tRNA synthetase includes alternative splicing. *J. Biol Chem.* **270**, 397–403 (1995).
4. Turpaev, K. T. *et al.* Alternative processing of the tryptophanyl-tRNA synthetase mRNA from interferon-treated human cells. *Eur J Biochem.* **240**, 732–737 (1996).
5. Shaw, A. C. *et al.* Mapping and identification of interferon gamma-regulated HeLa cell proteins separated by immobilized pH gradient two-dimensional gel electrophoresis. *Electrophoresis.* **20**, 984–993 (1999).
6. Wakasugi, K. *et al.* A human aminoacyl-tRNA synthetase as a regulator of angiogenesis. *Proc Natl Acad Sci USA.* **99**, 173–177 (2002).
7. Wakasugi, K., Nakano, T. & Morishima, I. Oxidative stress-responsive intracellular regulation specific for the angiostatic form of human tryptophanyl-tRNA synthetase. *Biochemistry.* **44**, 225–232 (2005).
8. Kise, Y. *et al.* A short peptide insertion crucial for angiostatic activity of human tryptophanyl-tRNA synthetase. *Nat Struct Mol Biol.* **11**, 149–156 (2004).
9. Yang, X. L., Schimmel, P. & Ewalt, K. L. Relationship of two human tRNA synthetases used in cell signaling. *Trends Biochem Sci.* **29**, 250–256 (2004).
10. Pajot, B., Sarger, C., Bonnet, J. & Garret, M. An alternative splicing modifies the C-terminal end of tryptophanyl-tRNA synthetase in murine embryonic stem cells. *J Mol Biol.* **242**, 599–603 (1994).
11. Kisselev, L., Frolova, L. & Haenni, A. L. Interferon inducibility of mammalian tryptophanyl-tRNA synthetase: new perspectives. *Trends Biochem Sci.* **18**, 263–267 (1993).
12. Fleckner, J., Martensen, P. M., Tolstrup, A. B., Kjeldgaard, N. O. & Justesen, J. Differential regulation of the human, interferon inducible tryptophanyl-tRNA synthetase by various cytokines in cell lines. *Cytokine.* **7**, 70–77 (1995).
13. Liu, J., Shue, E., Ewalt, K. L. & Schimmel, P. A new γ-interferon-inducible promoter and splice variants of an anti-angiogenic human tRNA synthetase. *Nucleic Acids Res.* **32**, 719–727 (2004).
14. Sajish, M. *et al.* Trp-tRNA synthetase bridges DNA-PKcs to PARP-1 to link IFN-γ and P53 signaling. *Nat Chem Biol.* **8**, 547–554 (2012).
15. Ogawa, S. *et al.* Crucial roles of mesodermal cell lineages in a murine embryonic stem cell-derived in vitro liver organogenesis system. *Stem Cells.* **23**, 903–913 (2005).
16. Tamai, M., Yamashita, A. & Tagawa, Y. Mitochondrial development of the *in vitro* hepatic organogenesis model with simultaneous cardiac mesoderm differentiation from murine induced pluripotent stem cells. *J. Biosci Bioeng.* **112**, 495–500 (2011).
17. Ewalt, K. L. & Schimmel, P. Activation of angiogenic signaling pathways by two human tRNA synthetases. *Biochemistry.* **41**, 13344–13349 (2002).
18. Yoshida, R., Imanishi, J., Oku, T., Kishida, T. & Hayaishi, O. Induction of pulmonary indoleamine 2,3-dioxygenase by interferon. *Proc Natl Acad Sci USA.* **78**, 129–132 (1981).
19. Yasui, H., Takai, K., Yoshida, R. & Hayaishi, O. Interferon enhances tryptophan metabolism by inducing pulmonary indoleamine 2,3-dioxygenase: Its possible occurrence in cancer patients. *Proc Natl Acad Sci USA.* **83**, 6622–6626 (1986).
20. Taylor, M. W. & Feng, G. Relationship between interferon-γ, indoleamine 2,3-dioxygenase, and tryptophan catabolism. *FASEB J.* **5**, 2516–2522 (1991).
21. Dai, X. & Zhu, B. T. Indoleamine 2,3-dioxygenase tissue distribution and cellular localization in mice: implications for its biological functions. *J. Histochem Cytochem.* **58**, 17–28 (2010).
22. Boasso, A., Herbeuval, J.-P., Hardy, A. W., Winkler, C. & Shearer, G. M. Regulation of indoleamine 2,3-dioxygenase and tryptophanyl-tRNA-synthetase by CTLA-4-Fc in human $CD4^+$ T cells. *Blood.* **105**, 1574–1581 (2005).
23. Platanias, L. C. Mechanism of type-I- and type-II-interferon-mediated signalling. *Nat Rev Immunol.* **5**, 375–386 (2005).
24. Saha, B., Prasanna, S. J., Chandrasekar, B. & Nandi, D. Gene modulation and immunoregulatory roles of interferon γ. *Cytokine.* **50**, 1–14 (2010).
25. Wakasugi, K. Human tryptophanyl-tRNA synthetase binds with heme to enhance its aminoacylation activity. *Biochemistry.* **46**, 11291–11298 (2007).
26. Wakasugi, K. Species-specific differences in the regulation of the aminoacylation activity of mammalian tryptophanyl-tRNA synthetases. *FEBS Lett.* **584**, 229–232 (2010).

Acknowledgments

This work was supported in part by the PRESTO program of Japan Science and Technology (JST) (to K.W.), the Life Science Foundation of Japan (to K.W.), and the Grant-in-Aids for Scientific Research on Innovative Areas (No. 23119003) (to Y.T.) and for Scientific Research (C) (No. 21570129) (to K.W.) from the Ministry of Education, Culture, Sports, Science and Technology of Japan.

Author contributions

M.M., T.T. and K.W. designed the experiments. M.M. and T.T. performed the experiments. M.T. and Y.T. prepared samples of murine ES cells and murine ES cell-derived *in vitro* liver tissue model. M.M. and K.W. analyzed the data and wrote the paper.

Additional information

Competing financial interests: The authors declare no competing financial interests.

How to cite this article: Miyanokoshi, M., Tanaka, T., Tamai, M., Tagawa, Y.-i. & Wakasugi, K. Expression of the rodent-specific alternative splice variant of tryptophanyl-tRNA synthetase in murine tissues and cells. *Sci. Rep.* **3**, 3477; DOI:10.1038/srep03477 (2013).